

# Unbiased approximation of posteriors via coupled particle Markov chain Monte Carlo

Willem van den Boom<sup>1,2</sup>, Ajay Jasra<sup>3</sup>, Maria De Iorio<sup>1,2,4,5</sup>,  
Alexandros Beskos<sup>5</sup>, and Johan G. Eriksson<sup>2,4</sup>

<sup>1</sup>National University of Singapore, Yale-NUS College

<sup>2</sup>Agency for Science, Technology and Research, Singapore Institute  
for Clinical Sciences

<sup>3</sup>King Abdullah University of Science and Technology, Computer,  
Electrical and Mathematical Sciences and Engineering division,  
Thuwal, Saudi Arabia

<sup>4</sup>National University of Singapore, Yong Loo Lin School of  
Medicine

<sup>5</sup>University College London, Department of Statistical Science, UK

## Abstract

Markov chain Monte Carlo (MCMC) is a powerful methodology for the approximation of posterior distributions. However, the iterative nature of MCMC does not naturally facilitate its use with modern highly parallelisable computation on HPC and cloud environments. Another concern is the identification of the bias and Monte Carlo error of produced averages. The above have prompted the recent development of fully (‘embarrassingly’) parallelisable unbiased Monte Carlo methodology based on couplings of MCMC algorithms. A caveat is that formulation of effective couplings is typically not trivial and requires model-specific technical effort. We propose couplings of sequential Monte Carlo (SMC) by considering adaptive SMC to approximate complex, high-dimensional posteriors combined with recent advances in unbiased estimation for state-space models. Coupling is then achieved at the SMC level and is, in general, not problem-specific. The resulting methodology enjoys desirable theoretical properties. We illustrate the effectiveness of the algorithm via application to two statistical models in high dimensions: (i) horseshoe regression; (ii) Gaussian graphical models.

**Keywords:** Adaptive sequential Monte Carlo; Coupling; Embarrassingly parallel computing; Gaussian graphical model; Particle filter; Unbiased MCMC

## Declarations

### Funding

This work is supported by the Singapore Ministry of Education Academic Research Fund Tier 2 (grant number MOE2019-T2-2-100) and the Singapore National Research Foundation under its Translational and Clinical Research Flagship Programme and administered by the Singapore Ministry of Health’s National Medical Research Council (grant number NMRC/TCR/004-NUS/2008; NMRC/TCR/012-NUHS/2014). Additional funding is provided by the Singapore Institute for Clinical Sciences, Agency for Science, Technology and Research.

### Conflicts of interest/Competing interests

The authors have no conflicts of interest to declare that relate to the content of this article.

### Availability of data and material

The data are confidential human subject data, thus are not available.

### Code availability

The scripts that produced the empirical results are available on <https://github.com/willemvandenboom/cpmcmc>.

## 1 Introduction

MCMC is a powerful methodology for the approximation of complex distributions. MCMC is intrinsically iterative and, while asymptotically unbiased, the size of the bias and the Monte Carlo error of generated estimates given a finite number of steps are typically difficult to quantify. These aspects of MCMC pose a challenge in high-dimensional applications and may not allow full exploitation of the computational potential of modern distributed-computing techniques. Recently, Jacob et al. (2020b) have proposed a method for unbiased MCMC estimation based on coupling of Markov chains, building on ideas by Glynn & Rhee (2014). The algorithm is embarrassingly parallelisable and the unbiasedness provides immediate quantification of the Monte Carlo error.

Let  $x \in \mathcal{X} \subseteq \mathbb{R}^{d_x}$ ,  $d_x \geq 1$ , denote the parameter,  $y \in \mathcal{Y} \subseteq \mathbb{R}^{d_y}$ ,  $d_y \geq 1$ , the data, and  $\pi(x)$  the density of the posterior of interest w.r.t. some dominating measure. The unbiased construction requires a pair of coupled ergodic Markov chains  $\{x(t-1), \bar{x}(t)\}$ ,  $t \geq 1$ , on  $\mathcal{X} \times \mathcal{X}$  with both chains having  $\pi(x)$  as equilibrium distribution. The coupling is such that  $x(t-1)$  and  $\bar{x}(t)$  have the same distribution for any  $t \geq 1$ , and the two chains meet at some random time  $\tau < \infty$  a.s. so that  $x(t) = \bar{x}(t)$  for  $t \geq \tau$ . Under standard conditions, the posterior expectation  $\pi(h) = \int_{\mathcal{X}} h(x) \pi(x) dx$  of a statistic  $h : \mathcal{X} \mapsto \mathbb{R}$  can be

obtained as  $\pi(h) = \lim_{t \rightarrow \infty} E[h\{x(t)\}]$  – all expectations are assumed to be finite. Writing the limit as a telescoping sum and using that fact that  $x(t-1)$ ,  $\bar{x}(t)$  admit the same law, gives for any fixed  $k \geq 0$  (Glynn & Rhee, 2014)

$$\begin{aligned} \pi(h) &= E[h\{x(k)\}] + \sum_{t=k+1}^{\infty} (E[h\{x(t)\}] - E[h\{x(t-1)\}]) \\ &= E[h\{x(k)\}] + \sum_{t=k+1}^{\infty} (E[h\{x(t)\}] - E[h\{\bar{x}(t)\}]) \\ &= E\left(h\{x(k)\} + \sum_{t=k+1}^{\tau-1} [h\{x(t)\} - h\{\bar{x}(t)\}]\right). \end{aligned}$$

We assume that the technical conditions that permit the exchange of summation and expectation in the last step hold in our setting. Thus, the quantity

$$\hat{h}_k = h\{x(k)\} + \sum_{t=k+1}^{\tau-1} [h\{x(t)\} - h\{\bar{x}(t)\}] \quad (1)$$

is an unbiased estimator of  $\pi(h)$ . The process  $\{\bar{x}(t)\}$  is typically initialised at  $\bar{x}(1) = x(0) \sim p_0$  for some law  $p_0$ . Both chains will evolve marginally according to the same MCMC chain with the posterior  $\pi(x)$  as invariant distribution, with a coupling applied for the joint transition  $[x(t), \bar{x}(t) \mid x(t-1), \bar{x}(t-1)]$ ,  $t \geq 2$ . We adopt this setting for the rest of the paper.

The specific construction of the coupled pair of MCMC chains  $\{x(t), \bar{x}(t)\}$ , can have a great impact on the variance of the deduced unbiased estimator. Devising effective coupling strategies for MCMC algorithms targeting a given posterior can be highly challenging. See for instance the construction of coupled MCMC for a horseshoe regression model in Biswas et al. (2020). We propose a coupled MCMC algorithm where the coupling mechanism is not specific to the posterior at hand by considering an augmented space.

The main contributions of this paper are summarised below:

- (i) We embed the inferential objective within a Feynman-Kac formulation, following the ideas of SMC in Del Moral et al. (2006). This is achieved by tempering the likelihood function  $p(y \mid x)$ , thus working with a sequence of posteriors  $p(x)p(y \mid x)^{\alpha_i}$  for a choice of reals  $\alpha_1 < \dots < \alpha_S < 1$ ,  $S \geq 1$ . The state-space model formulation is completed via the specification of ‘inner’ MCMC transitions with invariant distribution  $p(x)p(y \mid x)^{\alpha_i}$ ,  $1 \leq i \leq S$ . This construction leads to a target Feynman-Kac model, with density  $\Pi(x_{0:S})$  on the extended space  $\mathcal{X}^{S+1}$ , so that marginally  $x_S \sim \pi(x)$ . We apply the debiasing technique with target  $\Pi$  by making use of particle independent Metropolis-Hastings (PIMH) and conditional SMC (Andrieu et al., 2010) to produce ‘outer’ MCMC kernels with  $\Pi$  as invariant law. The key point is that coupling can now be attempted at the Metropolis-Hastings proposal or when resampling the particles, i.e. when

sampling from discrete-valued distributions with state-space of size  $N$ , with  $N \geq 1$  being the number of particles used by the SMC method. Note that Appendix B of Middleton et al. (2019) already delineates the main ideas behind coupled PIMH for general posteriors.

- (ii) Our main focus lies on delivering a methodology that is effective for high-dimensional models. The SMC framework is accompanied by a powerful toolkit for treating high-dimensional spaces, e.g. in the form of tempering and adaptation of tuning parameters. Beskos et al. (2014) show that, in given settings, the number of particles  $N$  needs to scale only linearly with  $d_x$ . We demonstrate the effectiveness of the proposed algorithm in two high-dimensional models involving horseshoe regression and Gaussian graphical models.
- (iii) For the Gaussian graphical model application, we devise inner MCMC transitions that sidestep the calculation of all involved intractable normalising constants.

Given the Feynman-Kac model formulation, our outer MCMC step can be thought of as synthesis of proposed steps in Middleton et al. (2019) and Jacob et al. (2020a). The focus of these works is unbiased approximation for the smoothing distribution of a state-space model; the high-dimensionality therein relates with the magnitude of  $S$ , whereas the dimension of  $\mathcal{X}$  is implicitly assumed low. We consider spaces  $\mathcal{X}$  of a much higher dimension than Middleton et al. (2019) and Jacob et al. (2020a), provide effective adaptation of the SMC, and propose a mixture strategy of conditional SMC and PIMH to improve mixing (as compared to PIMH) of the outer MCMC while retaining good coupling.

The structure of the paper is as follows. Section 2 introduces coupled particle MCMC for unbiased estimation for the case of a posterior given an inner MCMC step. Section 3 contains theoretical results for the meeting time  $\tau$  and the unbiased estimator in (1), deduced from the literature on coupled conditional SMC for state-space models (Lee et al., 2020). Section 4 applies the proposed general methodology to simulated data, including a case with horseshoe regression where a comparison with the MCMC coupling approach in Biswas et al. (2020) is carried out. Lastly, Section 5 considers Gaussian graphical models as an example where effective coupling of MCMC is not trivial.

## 2 Coupled particle MCMC

### 2.1 Theoretical background

Denote the parameter space by  $\mathcal{X}$  and the prior density on the parameter by  $p(x)$ . Let  $p(y | x)$  be the density of the data  $y$  given  $x$ . The posterior density follows from Bayes' rule as  $\pi(x) \propto p(x)p(y | x)$ . For any  $\alpha \in [0, 1]$ , we denote by  $\pi_\alpha(x)$  the tempered posterior proportional to  $p(x)p(y | x)^\alpha$ . Thus,  $\pi_0(x) = p(x)$  and  $\pi_1(x) = \pi(x)$ . All densities are assumed to be determined w.r.t. appropriate

reference measures. As our method involves adaptive SMC, we assume we can sample  $x$  from its prior  $p(x)$  and evaluate the likelihood  $p(y | x)$ . The method requires, for any  $\alpha \in (0, 1]$ , the construction of an MCMC step with  $\pi_\alpha(x)$  as its invariant distribution. For integers  $i \leq j$ , denote the range  $\{i, \dots, j\}$  by  $i:j$ . We use the standard semicolon notation for collections of variables, i.e.,  $x_{i:j} = \{x_i, \dots, x_j\}$  and  $x^{i:j} = \{x^i, \dots, x^j\}$ .

## 2.2 Feynman-Kac model & SMC sampler

The proposed unbiased estimation procedure builds on SMC. As a first step, we ‘adapt’ the SMC algorithm to the prior  $p(x)$  and likelihood  $p(y | x)$  under consideration. This is a preliminary step that determines the tempering constants and the inner MCMC steps, and thus the target Feynman-Kac model. The adaptation produces a sequence of  $S \geq 0$  temperatures,  $0 < \alpha_1 < \dots < \alpha_S < 1$ , corresponding to bridging distributions  $\pi_{\alpha_s}(x)$ ,  $s = 1, \dots, S$ . Here,  $S$  and temperatures  $\alpha_s$ ,  $s = 1, \dots, S$ , are chosen from this initial application of SMC with  $N_0 \geq 1$  particles, so that importance weights meet an effective sample size (ESS) threshold as, e.g., in Jasra et al. (2010). The adaptation also produces the number  $m_s$ ,  $s = 1, \dots, S$ , of iterations of a ‘simple’ MCMC kernel  $p_{\alpha_s}(dx' | x)$  that preserves  $\pi_{\alpha_s}(x)$ . For each  $s$ , we choose  $m_s$  via a criterion that requires sufficiently reduced sample correlation for pre- and post- scalar statistics  $f_j : \mathcal{X} \rightarrow \mathbb{R}$ ,  $j = 1, \dots$ , of the evolving particles. See Sections 4 and 5.5 for examples of such statistics for specific models, which in both cases include the log-likelihood  $f_1(x) = \log\{p(y | x)\}$ . Using a synthesis of  $m_s$  simple MCMC steps increases diversity among the particles  $x_s^{1:N_0}$  to avoid weight degeneracy. Kantas et al. (2014, Section 4.4) consider similar adaptation of  $m_s$ . Algorithm 1 summarizes the adaptive procedure where  $\widehat{\text{corr}}(\cdot, \cdot)$  in Step 2c denotes the sample correlation.

Once Algorithm 1 determines the Feynman-Kac model, then Algorithm 2 describes a standard SMC sampler corresponding to a bootstrap particle filter. Steps 2b and 3b of Algorithm 2 describe multinomial resampling. For our empirical results, we replace multinomial with systematic resampling, as the latter reduces variability (Chopin & Papaspiliopoulos, 2020, Section 9.7) and yields better mixing for the outer MCMC steps. Algorithm 8, Appendix A describes systematic resampling. Adaptive resampling (Chopin & Papaspiliopoulos, 2020, Section 10.2) further reduces the variance of the Monte Carlo estimates in our empirical results. That is, we only resample, i.e., apply Step 2b, if the ESS of the current weighted particle approximation falls below  $N\gamma$  for a  $\gamma \in [0, 1]$ .

Step 3b of Algorithm 2 is not required to approximate the posterior  $\pi(x)$  as the pair  $(w^{1:N}, x_S^{1:N})$  provides a weighted approximation. We include the step since conditional SMC will involve it. Section 2.4 discusses how Rao-Blackwellization enables the use of the weighted approximation in coupled particle MCMC.

---

**Algorithm 1** Adaptation of the Feynman-Kac model.

---

Input: Number of particles  $N_0$ , ESS and correlation thresholds  $\gamma_0, \zeta_0 \in [0, 1]$ .

1. Sample particles  $x_0^{1:N_0}$  independently from  $p(x)$ . Set  $s = 1$ ,  $\alpha_0 = 0$ .
2. Repeat while  $\alpha_{s-1} < 1$ :
  - (a) Compute weights  $w_s^i(\alpha) = p(y | x_{s-1}^i)^{\alpha - \alpha_{s-1}}$ ,  $i = 1, \dots, N$ , and find
$$\alpha_s = \min \left\{ \alpha \in (\alpha_{s-1}, 1] : 1 / \sum_{i=1}^{N_0} \{w_s^i(\alpha)\}^2 \leq \gamma_0 N_0 \right\}.$$
  - (b) Determine  $x_s^{1:N_0}$  by sampling with replacement from  $x_{s-1}^{1:N_0}$  with probabilities proportional to  $w_s^{1:N_0}(\alpha_s)$ .
  - (c) Let  $x_{s,k}^{1:N_0}$  denote the position of particles  $x_s^{1:N_0}$  after applying  $k \geq 1$  MCMC transitions  $p_{\alpha_s}(dx' | x)$  on each particle. Find

$$m_s = \min_{k \geq 1} \left\{ \max_j [\widehat{\text{corr}}\{f_j(x_s^{1:N_0}), f_j(x_{s,k}^{1:N_0})\}] \leq \zeta_0 \right\}.$$

With an abuse of notation, let  $x_s^{1:N_0}$  now be the particles after the application of  $m_s$  MCMC steps.

- (d) Set  $s = s + 1$ .

Output: Temperatures  $0 < \alpha_1 < \dots < \alpha_S < 1$ , number of MCMC steps  $m_{1:S}$ .

---

**Algorithm 2** SMC sampler.

---

Input: Number of particles  $N$ , temperatures  $0 = \alpha_0 < \dots < \alpha_S < 1$ , number of MCMC steps  $m_{1:S}$ .

1. Sample  $N$  particles  $x_0^{1:N}$  independently from  $\pi_{\alpha_0}(x) = p(x)$ .
2. For  $s = 1, \dots, S$ :
  - (a) Compute weights  $w_s^i = p(y | x_{s-1}^i)^{\alpha_s - \alpha_{s-1}}$ ,  $i = 1, \dots, N$ .
  - (b) Determine  $x_s^{1:N}$  by sampling with replacement from  $x_{s-1}^{1:N}$  with probabilities proportional to  $w_s^{1:N}$ .
  - (c) For each particle in  $x_s^{1:N}$ , apply  $m_s$  MCMC transitions  $p_{\alpha_s}(dx' | x)$ . With an abuse of notation, let  $x_s^{1:N}$  be the particles after application of the MCMC steps.
3. (a) Compute weights  $w^i = p(y | x_S^i)^{1 - \alpha_S}$ ,  $i = 1, \dots, N$ .
- (b) Determine  $x^{1:N}$  by sampling with replacement from  $x_S^{1:N}$  with probabilities proportional to  $w^{1:N}$ .

Output: Set of particles  $x^{1:N}$  that approximate the posterior  $\pi(x)$ .

---

### 2.3 Coupling of particle MCMC

Having specified an SMC sampler, we derive a coupled particle MCMC algorithm. The outer MCMC step is constructed from the SMC sampler. Specifically, we borrow ideas from the particle filtering literature and define a coupling strategy of the MCMC step as a mixture of the coupled PIMH in Middleton et al. (2019, Algorithm 3) and the coupled conditional particle filters in Jacob et al. (2020a, Algorithm 2). PIMH and conditional SMC (Andrieu et al., 2010, Section 2.4) provide MCMC steps on the extended state space  $x_{0:S} \in \mathcal{X}^{S+1}$  based on Algorithm 2. The invariant law on  $\mathcal{X}^{S+1}$  of such MCMC has  $\pi(x)$  as marginal distribution on  $x_S \in \mathcal{X}$  (Andrieu et al., 2010, Theorems 2, 5). Therefore, the resulting MCMC algorithm can be run for two coupled chains to provide unbiased Monte Carlo estimation per (1). The added machinery of SMC provides more ways to couple the MCMC compared to using a less elaborate MCMC algorithm for sampling from the posterior  $\pi(x)$ .

Coupled PIMH results in smaller meeting times  $\tau$  and worse mixing of the MCMC chain than conditional SMC in our experiments. The meeting times and the MCMC mixing both affect the variance of the resulting unbiased estimators. The empirical results show that neither PIMH nor conditional SMC yields universally better performance. We thus consider a mixture of them as the outer MCMC step. Next, we describe coupled PIMH and coupled conditional SMC separately.

---

**Algorithm 3** Coupled PIMH step.

---

Input: Current states  $x_{0:S}$  and  $\bar{x}_{0:S}$  with their corresponding SMC estimates  $Z$  and  $\bar{Z}$  of the marginal likelihood.

1. Sample  $\tilde{x}_{0:S}$  and  $\tilde{Z}$  using Algorithm 2 as the proposal for both chains:
  - (a) Set  $\tilde{x}_S$  equal to  $x^1$  from the output of Algorithm 2.
  - (b) For  $s = S - 1, \dots, 0$ , set  $\tilde{x}_s$  equal to the element in  $x_s^{1:N}$  which generated  $\tilde{x}_{s+1}$  per Step 2b of Algorithm 2. In other words,  $\tilde{x}_s$  is the ancestor of  $\tilde{x}_{s+1}$ .
  - (c) Compute the corresponding marginal likelihood estimate  $\tilde{Z}$  from the weights in Algorithm 2 as detailed in Del Moral et al. (2006, Section 3.2.1).
2. Perform two coupled Metropolis-Hastings accept-reject steps:
  - (a) Sample  $U \sim \mathcal{U}(0, 1)$ .
  - (b) If  $U < \tilde{Z}/Z$ , then set  $x_{0:S} = \tilde{x}_{0:S}$  and  $Z = \tilde{Z}$ .
  - (c) If  $U < \tilde{Z}/\bar{Z}$ , then set  $\bar{x}_{0:S} = \tilde{x}_{0:S}$  and  $\bar{Z} = \tilde{Z}$ .

Output: Updated states  $x_{0:S}$  and  $\bar{x}_{0:S}$  with corresponding  $Z$  and  $\bar{Z}$  such that the invariant distributions of  $x_S$  and  $\bar{x}_S$  are the posterior  $\pi(x)$ .

---

## Coupled PIMH

Algorithm 3 details the coupled PIMH update. SMC provides an unbiased estimate  $Z$  of the marginal likelihood corresponding to the Feynman-Kac formulation. The unbiasedness enables the use of independent Metropolis-Hastings which is coupled by using the same proposal and the same uniform random variable  $U$  in the accept-reject step across both chains. Then, both chains meet as soon as they both accept the proposal in Step 2 at the same MCMC iteration.

---

### Algorithm 4 Coupled conditional SMC step.

---

Input: Current states  $x_{0:S}$  and  $\bar{x}_{0:S}$

1. Set  $x_s^1 = x_s$  and  $\bar{x}_s^1 = \bar{x}_s$  for  $s = 0, \dots, S$ .
2. Sample  $N - 1$  particles  $x_0^{2:N}$  independently from  $\pi_{\alpha_0}(x) = p(x)$ .
3. Set  $\bar{x}_0^i = x_0^i$  for  $i = 2, \dots, N$ .
4. For  $s = 1, \dots, S$ :
  - (a) Compute weights  $w_s^i = p(y | x_{s-1}^i)^{\alpha_s - \alpha_{s-1}}$ ,  $\bar{w}_s^i = p(y | \bar{x}_{s-1}^i)^{\alpha_s - \alpha_{s-1}}$ ,  $i = 1, \dots, N$ .
  - (b) Determine  $x_s^{2:N}$  and  $\bar{x}_s^{2:N}$  by coupled resampling (Algorithm 5) with replacement from  $x_{s-1}^{1:N}$  and  $\bar{x}_{s-1}^{1:N}$  with probabilities proportional to  $w_s^{1:N}$  and  $\bar{w}_s^{1:N}$ , respectively.
  - (c) Update  $x_s^i$  and  $\bar{x}_s^i$  by taking  $m_s$  coupled MCMC steps which are invariant w.r.t.  $\pi_{\alpha_s}(x)$  for  $i = 2, \dots, N$ .
5. (a) Compute weights  $w^i = p(y | x_S^i)^{1 - \alpha_S}$ ,  $\bar{w}^i = p(y | \bar{x}_S^i)^{1 - \alpha_S}$ ,  $i = 1, \dots, N$ .
- (b) Determine  $x_{0:S}$  and  $\bar{x}_{0:S}$  by coupled resampling (Algorithm 5) with replacement from  $\{x_{0:S}^i\}_{i=1}^N$  and  $\{\bar{x}_{0:S}^i\}_{i=1}^N$  with probabilities proportional to  $w^{1:N}$  and  $\bar{w}^{1:N}$ , respectively.

Output: Updated states  $x_{0:S}$  and  $\bar{x}_{0:S}$  such that the invariant distributions of  $x_S$  and  $\bar{x}_S$  are the posterior  $\pi(x)$ .

---

## Coupled conditional SMC

Algorithm 4 details the coupled conditional SMC update. The resampling of the particles in Steps 4b and 5b forms the main source of coupling across the two chains  $x_{0:S}$  and  $\bar{x}_{0:S}$ . As in Jacob et al. (2020a) and Lee et al. (2020), we consider Algorithm 5 for the coupled resampling. Earlier applications of Algorithm 5 can be found in Chopin & Singh (2015) for theoretical analysis of conditional SMC and Jasra et al. (2017) for multilevel particle filtering. The algorithm samples from two discrete distributions such that the resulting two indices are equal with maximum probability (Jasra et al., 2017, Section 3.2).



---

**Algorithm 5** (Chopin & Singh, 2015, Section 3.1; Jasra et al., 2017, Algorithm 1) Coupled resampling.

---

Input: Probability vectors  $p_{1:N}$  and  $\bar{p}_{1:N}$ .

1. Compute  $p_i^{\min} = \min(p_i, \bar{p}_i)$  for  $i = 1, \dots, N$ .
2. (a) With probability  $a = \sum_{i=1}^N p_i^{\min}$ :
  - i. Draw  $i$  according to the law on  $1:N$  defined by the probability vector  $p_{1:N}^{\min}/a$ .
  - ii. Let  $\bar{i} = i$ .
- (b) With probability  $1 - a$ , draw  $i$  and  $\bar{i}$  according to the laws defined by the probability vectors  $(p_{1:N} - p_{1:N}^{\min})/(1 - a)$  and  $(\bar{p}_{1:N} - p_{1:N}^{\min})/(1 - a)$ , respectively.

Output: Samples  $i$  and  $\bar{i}$  which are distributed according to  $p_{1:N}$  and  $\bar{p}_{1:N}$ , respectively, and for which the probability of  $i = \bar{i}$  is maximized.

---

We use systematic resampling (Algorithm 8, Appendix A) for the empirical results. Thus, we require a coupling for it. Chopin & Singh (2015) derive a modification of systematic resampling for use with conditional SMC. We propose a coupling of this conditional systematic resampling for Step 4b of Algorithm 4. Appendix A details these algorithms.

Step 4c of Algorithm 4 involves a coupling of the MCMC update for  $\pi_{\alpha_s}(x)$  across two chains. A coupling of two MCMC updates is a joint MCMC update with as marginals the initially given MCMC update. The coupling should at least be ‘faithful’ (Rosenthal, 1997), i.e., it sustains any meeting of the chains. That is, if  $x_s^i = \bar{x}_s^i$  initially, then that should still be true after the coupled MCMC updates of  $x_s^i$  and  $\bar{x}_s^i$ . One way to achieve this minimal coupling is by using the same seed for the pseudorandom number generators in both MCMC updates. Better coupling of MCMC updates will further improve the coupling of our method.

## 2.4 Unbiased Monte Carlo approximation

Algorithm 6 specifies the coupled MCMC algorithm resulting from a mixture of Algorithms 3 and 4 with mixture weight  $\rho$ . It provides chains  $\{x(t)\}_{t=1}^T$  and  $\{\bar{x}(t)\}_{t=1}^T$  which can be used to estimate expectations w.r.t. the posterior  $\pi(x)$  via ergodic averages. By construction,  $x(t-1)$  and  $\bar{x}(t)$  have the same distribution for any  $t \geq 1$ . Also, they meet at some time  $\tau$  which is almost surely finite under the conditions given in Section 3 for  $\rho = 0, 1$ . This enables unbiased Monte Carlo estimation of  $\pi(h)$  as described in (1).

Middleton et al. (2019, Section 2.2) propose the initialization in Step 2a. It enables  $\tau = 1$  as  $x_{0:S}(1) = \bar{x}_{0:S}(1)$  if the PIMH step accepts. Moreover,  $\Pr(\tau = 1) \geq 1/2$  if only PIMH is used, i.e.  $\rho = 1$  (Middleton et al., 2019, Proposition 8). Note that a high  $\Pr(\tau = 1)$  does not necessarily result in low variance

---

**Algorithm 6** Coupled particle MCMC.

---

Input: Minimum number of MCMC steps  $l$  and probability  $\rho$  of using PIMH

1. Initialize  $x_{0:S}(0)$  by running the SMC algorithm as per Step 1 of Algorithm 3.
2. (a) With probability  $\rho$ , draw  $x_{0:S}(1) | x_{0:S}(0)$  according to the PIMH algorithm, for instance by running Algorithm 3 with  $x_{0:S} = \bar{x}_{0:S} = x_{0:S}(0)$ , and set  $\bar{x}_{0:S}(1)$  equal to the proposal  $\tilde{x}_{0:S}$  from this PIMH.  
(b) With probability  $1 - \rho$ , set  $\bar{x}_{0:S}(1) = x_{0:S}(0)$  and draw  $x_{0:S}(1) | x_{0:S}(0)$  according to the conditional SMC algorithm, for instance by running Algorithm 4 with  $x_{0:S} = \bar{x}_{0:S} = x_{0:S}(0)$ .
3. Let  $\tau = \inf\{\tau \geq 1 \mid x_{0:S}(\tau) = \bar{x}_{0:S}(\tau)\}$  and  $T = \max(\tau, l)$ . For  $t = 2, \dots, T$ , draw  $x_{0:S}(t) | x_{0:S}(t-1)$  and  $\bar{x}_{0:S}(t) | \bar{x}_{0:S}(t-1)$  using the coupled PIMH step in Algorithm 3 with probability  $\rho$  and the coupled conditional SMC step in Algorithm 4 with probability  $1 - \rho$ .

Output: Chains  $\{x(t)\}_{t=1}^T = \{x_S(t)\}_{t=1}^T$  and  $\{\bar{x}(t)\}_{t=1}^T = \{\bar{x}_S(t)\}_{t=1}^T$  that meet.

---

Monte Carlo estimation. For instance, consider  $\bar{x}(1) = x(0)$  and let  $x(1) | x(0)$  follow a Metropolis-Hastings update. Then,  $\Pr(\tau = 1) = \Pr\{\bar{x}(1) = x(1)\}$  corresponds to the Metropolis-Hastings rejection probability which should not be too high for effective MCMC.

The unbiasedness of the estimator  $\hat{h}_k$  in (1) enables embarrassingly parallel computation for independent estimates. Consider  $R$  independent runs of Algorithm 6 resulting in  $R$  independent copies of the estimator denoted by  $\hat{h}_k^r$ ,  $r = 1, \dots, R$ . Then,  $R^{-1} \sum_r \hat{h}_k^r$  is an unbiased estimator of  $\pi(h)$ . Its variance decreases linearly in  $R$  and can be estimated by its empirical variance. Moreover, the unbiasedness and independence of the  $R$  estimators enables the construction of confidence intervals for  $\pi(h)$  which are exact as  $R \rightarrow \infty$  per the central limit theorem.

Jacob et al. (2020a, Section 4) provide improvements to the unbiased estimator  $\hat{h}_k$  in (1) that reduce its variance for each run of Algorithm 6. Firstly, one can average over different  $k$  since  $\hat{h}_k$  is unbiased for any  $k \geq 1$ . For any positive integers  $k$  and  $l$  with  $k \leq l$ , this results in the unbiased estimator

$$\begin{aligned} \bar{h}_k^l &= \frac{1}{l-k+1} \sum_{q=k}^l \hat{h}_q \\ &= \frac{1}{l-k+1} \sum_{q=k}^l \left( h\{x(q)\} + \sum_{t=q+1}^{\tau-1} [h\{x(t)\} - h\{\bar{x}(t)\}] \right) \\ &= \frac{1}{l-k+1} \sum_{t=k}^l h\{x(t)\} + \sum_{t=k+1}^{\tau-1} \frac{\min(l-k+1, t-k)}{l-k+1} [h\{x(t)\} - h\{\bar{x}(t)\}], \end{aligned} \tag{2}$$

where the penultimate term is an ergodic average and the last term is a bias correction. The ergodic average  $(l - k + 1)^{-1} \sum_{t=k}^l h\{x(t)\}$  discards the first  $k - 1$  steps in the chain  $\{x(t)\}_{t=1}^T$  as burn-in iterations and uses  $l - k + 1$  recorded iterations.

As  $k$  increases, the variance of the bias correction, the last term in (2), decreases. Moreover, the bias correction equals zero for  $k \geq \tau - 1$ . Nonetheless, it is suboptimal to set  $k$  very large as that increases the variance of the ergodic average similar to when discarding too many iterations as burn-in in MCMC. One can pick  $k$  as a high percentile of the empirical distribution of the meeting time  $\tau$  from multiple runs of Algorithm 6. Alternatively, the empirical variance of  $\hat{h}_k^l$  can be minimized via a grid search over  $k$  (Middleton et al., 2019, Appendix B.2), at the price of losing the unbiasedness of  $\hat{h}_k^l$ . The parameter  $l$  can be set to a large value within computational constraints as a larger  $l$  reduces the variance of the unbiased estimator in (2).

A second variance reduction technique is Rao-Blackwellization of the estimator  $\hat{h}_k$  over the weighted particle approximation from SMC. So far, we have considered only the single particle selected by Algorithm 3 or Step 5b of Algorithm 4. It is more efficient to use all  $N$  particles via the weighted approximations defined by the pairs  $(w^{1:N}, x_S^{1:N})$  and  $(\bar{w}^{1:N}, \bar{x}_S^{1:N})$ . Specifically,  $h\{x(t)\}$  and  $h\{\bar{x}(t)\}$  in (1) and (2) can be replaced by  $\sum_{i=1}^N w^i(t) h\{x_S^i(t)\} / \sum_{i=1}^N w^i(t)$  and  $\sum_{i=1}^N \bar{w}^i(t) h\{\bar{x}_S^i(t)\} / \sum_{i=1}^N \bar{w}^i(t)$ , respectively, where the weights and particles are given in Step 3b of Algorithm 2 or Step 5b of Algorithm 4.

### 3 Theoretical properties

Existing analysis of coupled conditional SMC applies to our context which aims to approximate the posterior  $\pi(x)$ . Building on Lee et al. (2020), we derive results for Algorithm 6 with  $\rho = 0$ , such that only conditional SMC is used. Appendix B contains the proofs which mostly consist of a mapping from the smoothing problem considered in Lee et al. (2020) to our context of posterior approximation. That mapping results in the following assumptions.

**Assumption 1.** *The likelihood is bounded. That is,  $\sup_{x \in \mathcal{X}} p(y | x) < \infty$  for the observed data  $y$ .*

**Assumption 2.** *The statistic  $h : \mathcal{X} \rightarrow \mathbb{R}$ , as in (1), is bounded. That is,  $\sup_{x \in \mathcal{X}} |h(x)| < \infty$ .*

Many models satisfy Assumption 1, including the Gaussian graphical model in Section 5. The likelihood from linear regression in Section 4.2 violates it if the number of predictors is greater than the number of observations. The assumption relates to the boundedness of potential functions in the SMC literature, which is a common assumption (Del Moral, 2004, Section 2.4.1). Andrieu et al. (2018, Theorem 1) show that Assumption 1 is essentially equivalent to uniform ergodicity of the Markov chains produced by conditional SMC in Algorithm 6 with  $\rho = 0$ .

Jacob et al. (2020a, Section 3) establish unbiasedness and finite variance of the estimator  $\hat{h}_k$  in (1), like we do, but without the boundedness in Assumption 2 and instead use an assumption jointly on  $h(x)$  and the Markov chain generated by conditional SMC. The simpler and more restrictive Assumption 2 provides a bound on the variance of  $\hat{h}_k$  in terms of the number of particles  $N$  in Proposition 2.

Assumptions 1 and 2 imply Assumptions 6 and 4 of Middleton et al. (2019), respectively. Therefore, the estimator  $\hat{h}_k$  from Algorithm 8 with  $\rho = 1$ , such that it uses only PIMH, is unbiased and has finite variance, and  $\tau < \infty$  almost surely per Proposition 8 of Middleton et al. (2019) and its proof under Assumptions 1 and 2.

**Proposition 1.** *Suppose Assumption 1 holds. Consider Algorithm 6 with  $\rho = 0$ . Then, for any number of temperatures  $S \geq 0$ , there exists a  $c < \infty$  such that for any number of particles  $N \geq 2$  and any initial  $(x_{0:S}, \bar{x}_{0:S})$ , we have:*

- (i)  $\Pr(x'_{0:S} = \bar{x}'_{0:S}) \geq N/(N+c)$  where  $(x'_{0:S}, \bar{x}'_{0:S})$  are distributed per coupled conditional SMC in Algorithm 4.
- (ii)  $\tau < \infty$  almost surely.
- (iii) The average meeting time  $E(\tau) \leq 2 + c/N$ .

Proposition 1 contains no conditions on the quality of the coupling of the MCMC steps in Step 4c of Algorithm 4. This confirms that the SMC machinery by itself enables coupling and thus unbiased estimation for the posterior  $\pi(x)$ . Moreover, the meeting time  $\tau$  can be made equal to 2 with arbitrarily high probability by increasing the number of particles  $N$ .

Whether a sufficient increase of  $N$  is practicable depends on the SMC sampler in Algorithm 2 which we adapt to  $\pi(x)$ . For instance, under additional assumptions, Theorem 9 from Lee et al. (2020) states that the meeting probability  $\Pr(x'_{0:S} = \bar{x}'_{0:S})$  does not vanish if the number of particles scales as  $N = \mathcal{O}(2^S S)$  where  $S$  is the number of temperatures.

**Proposition 2.** *Suppose Assumptions 1 and 2 hold. Consider the estimator  $\hat{h}_k$  of  $\pi(h)$  in (1) where the chains  $x(t)$  and  $\bar{x}(t)$  are generated by Algorithm 6 with  $\rho = 0$ . Denote the expectation and variance w.r.t. the resulting distribution on  $\{x(t), \bar{x}(t)\}_{t=1}^T$  by  $\hat{E}(\cdot)$  and  $\hat{\text{var}}(\cdot)$ , respectively. Then, for any number of temperatures  $S \geq 0$ , we have:*

- (i) For any  $k \geq 1$ ,  $\hat{E}(\hat{h}_k) = \pi(h)$  and  $\hat{\text{var}}(\hat{h}_k) < \infty$ .
- (ii) There exists a  $c < \infty$  such that for any  $k \geq 1$  and for any number of particles  $N \geq 2$  in Algorithm 4,

$$\begin{aligned} & |\hat{\text{var}}(\hat{h}_k) - \text{var}\{h(x) \mid y\}| \\ & \leq 16 \left(\frac{N+c}{N}\right)^2 \left(\frac{c}{N+c}\right)^{k/2} \sup_{x \in \mathcal{X}} |h(x) - \pi(h)|. \end{aligned}$$

Proposition 2 confirms the unbiasedness of  $\hat{h}_k$ . Moreover, the variance penalty resulting from the bias correction sum in (1) vanishes as  $N \rightarrow \infty$  or  $k \rightarrow \infty$ . The latter confirms the role of  $k$  as the number of burn-in iterations in the MCMC estimation. The constant  $c$  in Proposition 2 is the same as in Proposition 1.

## 4 Simulation studies

In all our applications, Algorithm 1 adapts the Feynman-Kac model with  $N_0 = 10^4$  particles, an ESS threshold of  $\gamma_0 = 0.8$  to determine  $\alpha_{0:S}$  and a correlation threshold of  $\zeta_0 = 0.95$  for  $m_{0:S}$ . Subsequent use of SMC algorithms applies adaptive resampling with  $\gamma = 0.5$ . All empirical results in this paper use Rao-Blackwellization when computing  $\bar{h}_k^l$ .

### 4.1 Mixture of Gaussians

The first set of empirical results derive from the Bayesian model and SMC considered in Section B.2 of Middleton et al. (2019). The likelihood is

$$p(y | x) = \prod_{i=1}^{d_y} \frac{1}{d_x} \sum_{j=1}^{d_x} \mathcal{N}(y_i | x_j, 1)$$

and the prior is uniform over the hypercube  $[-10, 10]^{d_x}$ . We consider  $d_x = 2$  and  $d_y = 100$ , and simulate the data  $y$  from  $p(y | x)$  with the true values  $x^* = (-3, 0)^T$ . Then, the posterior  $\pi(x) \propto p(x)p(y | x)$  is multimodal. The inner MCMC step is a random walk Metropolis-Hastings step with a Gaussian distribution with identity covariance as proposal. We couple this MCMC across two chains by using the same seed for the pseudorandom number generator in each of the two MCMC updates, which results in a common random number coupling.

The univariate statistics used to determine  $m_{1:S}$  are the log-likelihood  $f_1(x) = \log\{p(y | x)\}$  and the  $L_2$  norm  $f_2(x) = \|x\|$ . We aim to estimate  $\pi(h)$  for  $h(x) = x_1 + x_2 + x_1^2 + x_2^2$ . We run Algorithm 6 1,024 times for each  $\rho = 0, 1/2, 1$  with a minimum number of steps  $l = 10^4$  and  $N = 25$  particles. The integrated autocorrelation time for each run based on the chain  $\sum_{i=1}^N w^i(t) h\{x_S^i(t)\} / \sum_{i=1}^N w^i(t)$ ,  $t = l/2, \dots, l$ , computed using the R package `LaplacesDemon` (Statisticat, LLC., 2020), gauges the mixing of the outer MCMC.

We consider the product ‘ $\hat{\text{var}}(\bar{h}_k^l) \times \text{time}$ ’ of the empirical variance of  $\bar{h}_k^l$  and the average computation time to obtain one  $\bar{h}_k^l$  across the 1,024 runs. This product captures the tradeoff between quantity and quality of unbiased estimates: the variance of the average of independently and identically distributed estimates  $\bar{h}_k^l$  is proportional to  $\hat{\text{var}}(\bar{h}_k^l)$  and inversely proportional to the number of estimates. The number of estimates is in turn inversely proportional to the average computation time when working with a fixed computational budget.

We compute ‘ $\text{v\hat{a}r}(\bar{h}_k^l) \times \text{time}$ ’ for  $l = 1, \dots, 10^4$  where  $k \leq l$  is set for each  $l$  such that  $\text{v\hat{a}r}(\bar{h}_k^l)$  is minimized.

Figure 1 shows that coupling times are lowest for Algorithm 6 with PIMH while mixing of the outer MCMC step is best with conditional SMC. A mixed set-up with  $\rho = 1/2$  provides a tradeoff between these extremes. The ‘ $\text{v\hat{a}r}(\bar{h}_k^l) \times \text{time}$ ’ is lowest for conditional SMC owing to its better mixing but only if Algorithm 6 is run for sufficiently more iterations than the largest meeting times.

## 4.2 Horseshoe regression

### Background

Biswas et al. (2020) recently proposed a coupling of an MCMC step for horseshoe regression (Carvalho et al., 2009). This section compares the coupling and its resulting unbiased estimation with the proposed coupled particle MCMC in Algorithm 6.

We consider the standard likelihood for linear regression

$$p(y | x) = \mathcal{N}(y | W\beta, \sigma^2 I_n)$$

where  $y$  is an  $d_y$ -dimensional vector of observations,  $W$  is a  $d_y \times p$  design matrix and  $\sigma^2$  is the error variance. The main object of inference is the  $p$ -dimensional coefficient vector  $\beta$ . The horseshoe prior on  $\beta$  is one of the most popular global-local shrinkage priors which provide state-of-the-art Bayesian variable selection (Bhadra et al., 2019). It is defined by  $\beta_j | \sigma^2, \xi, \eta_j \sim \mathcal{N}\{0, \sigma^2 / (\xi \eta_j)\}$  independently for  $j = 1, \dots, p$  where  $\xi$  is a global precision parameter with prior  $\sqrt{\xi} \sim C^+(0, 1)$  and  $\eta_j$  is a local precision parameter with prior  $\sqrt{\eta_j} \sim C^+(0, 1)$  independently for  $j = 1, \dots, p$ . Here,  $C^+(0, 1)$  denotes the standard half-Cauchy distribution. That is, if  $t \sim C^+(0, 1)$ , then the density of  $t$  is  $p(t) = 2 / \{\pi(1+t^2)\}$  for  $t > 0$  and zero otherwise.

We follow the simulation set-up of Biswas et al. (2020, Section 3). The gamma prior  $1/\sigma^2 \sim \text{Gamma}(1, 1)$  completes the Bayesian model specification. The elements of the matrix  $W$  are sampled independently from the standard Gaussian distribution. We draw  $y \sim \mathcal{N}(W\beta_*, \sigma_*^2 I_n)$  for some true  $\beta_*$  and true error variance  $\sigma_*^2$ . We set  $\sigma_*^2 = 8$ ,  $d_y = 100$ ,  $p = 20$ ,  $\beta_{*,j} = 2^{(9-j)/4}$  for  $j = 1, \dots, 10$  and  $\beta_{*,j} = 0$  for  $j = 11, \dots, p$ .

### Coupled particle MCMC for horseshoe regression

Algorithm 1 from Biswas et al. (2020) provides the inner MCMC step that is invariant w.r.t. the posterior  $\pi(x)$ . Here,  $x = (\beta, \eta, \sigma^2, \xi)$  since the MCMC provides a Markov chain on these parameters jointly. Additionally, our method requires an inner MCMC step that is invariant w.r.t.  $\pi_\alpha(x) \propto p(x) p(y | x)^\alpha$ , e.g., Step 2c of Algorithm 2. Here,  $p(y | x)^\alpha$  equals  $p(y | x)$  with  $n$ ,  $y$  and  $W$  replaced by  $\alpha n$ ,  $\sqrt{\alpha} y$  and  $\sqrt{\alpha} W$ , respectively. Therefore, the required MCMC for  $\pi_\alpha(x)$  follows from making this same substitution in the MCMC for  $\pi(x)$ .

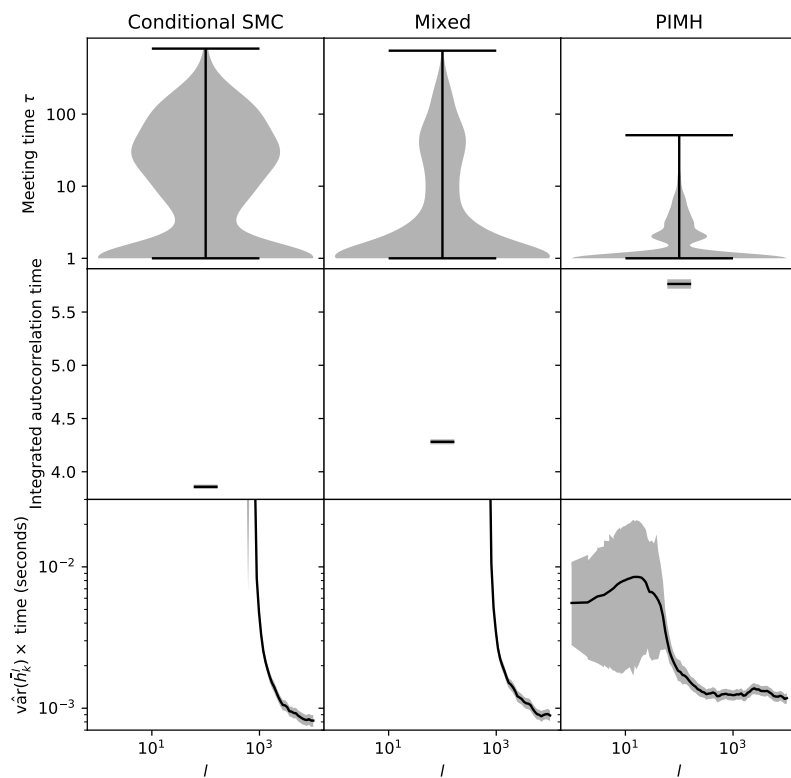


Figure 1: Results from Algorithm 6 with  $\rho = 0$  (conditional SMC),  $\rho = 1/2$  (mixed) and  $\rho = 1$  (PIMH) for the simulation with a mixture of Gaussians. The top row contains violin plots of  $\log(\tau)$ . The bottom two rows show the integrated autocorrelation time and  $\hat{\text{var}}(\bar{h}_k^l) \times \text{time}$  as a function of  $l$  with their means and 95% bootstrapped confidence intervals in black and gray, respectively.

The univariate statistics used to determine the number of MCMC steps  $m_{1:s}$  are the log-likelihood  $f_1(x) = \log\{p(y | x)\}$  and the number of elements in  $\beta$  that have an absolute value greater than 0.01,  $f_2(x) = \sum_{j=1}^p |\beta_j| > 0.01$ . The latter is a rough measure of the number of variables that are selected into the model at that MCMC iteration. Algorithm 1 produces  $m_s = 1$  for all  $s$ . This confirms the effectiveness of the MCMC algorithm which has favourable theoretical properties per Biswas et al. (2020, Section 2.2). We compare the estimation of the posterior expectation of  $h(x) = \beta_{10} + \beta_{10}^2$  obtained from different algorithms.

## Results

We compare the results from coupled particle MCMC (Algorithm 6) with  $\rho = 1$  and  $\rho = 0.9$  using  $N = 25$  particles to the two-scale coupling of Biswas et al. (2020, Section 3.2) which provides a direct coupling of the MCMC algorithm that we use as the inner MCMC step. Algorithm 6 with  $\rho = 0.9$  uses this same coupling of the inner MCMC when calling Algorithm 4. The three coupled MCMCs are run 128 times each for  $l = 10^3$  iterations. Figure 2 presents the results analogous to Figure 1.

Coupled particle MCMC meets in fewer iterations than the coupled MCMC from Biswas et al. (2020). Nonetheless, coupled particle MCMC takes more computation time to achieve the same estimation accuracy. One reason for this is the mixing of the coupled MCMC as shown in Figure 2 with a much higher integrated autocorrelation time for coupled particle MCMC. Another reason is that the computational cost of the outer particle MCMC step in Algorithm 6 is much higher than that of a single inner MCMC step. This increased cost of particle methods can be alleviated by parallelizing across particles if the main concern is elapsed real time rather than cumulative CPU time across CPU cores. The results for ‘ $\text{var}(\bar{h}_k^l) \times \text{time}$ ’ show that it is not sufficient to only consider meeting times when assessing coupled MCMC for unbiased estimation if the MCMC algorithms compared differ in mixing or computational cost.

Figure 2 suggests that conditional SMC mixes better than PIMH but results in a worse coupling of the outer MCMC. Here, the improvement over PIMH in mixing does not outweigh the worse coupling of conditional SMC at  $l = 10^3$  outer MCMC iterations.

## 5 Application: Gaussian graphical models

### 5.1 Model

We consider Gaussian graphical models (Dempster, 1972; Lauritzen, 1996) as an example in high-dimensional discrete spaces. Coupling of MCMC kernels on the original non-extended space appears highly challenging. In general, generation of unbiased estimators for posterior expectations in this context is a major undertaking, and it is attempted – to the best of our knowledge – for the first time in this work. We allow the graphs to be non-decomposable, and present methodology that sidesteps approximation of intractable normalising constants.



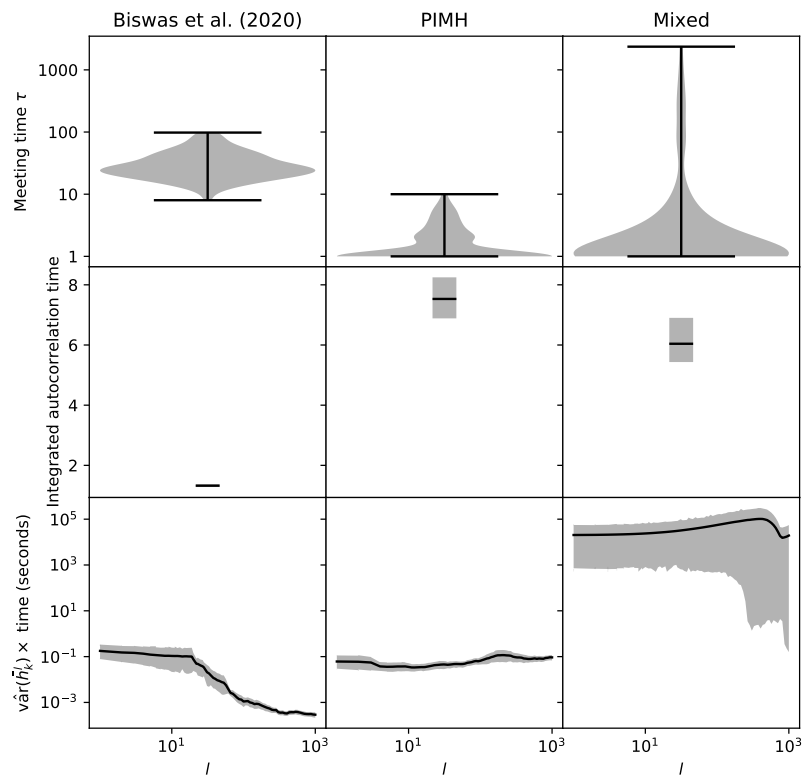


Figure 2: Results from the coupled MCMC from Biswas et al. (2020) (left), and Algorithm 6 with  $\rho = 1$  (PIMH) and  $\rho = 0.9$  (mixed) for the horseshoe regression simulation. The top row contains violin plots of  $\log(\tau)$ . The bottom two rows show the integrated autocorrelation time and  $\text{var}(\hat{h}_k^l) \times \text{time}$  as a function of  $l$  with their means and 95% bootstrapped confidence intervals in black and gray, respectively.

The object of inference is an undirected graph  $G = (V, E)$  defined by a set of nodes  $V = \{1, \dots, p\}$ ,  $p \geq 1$ , and a set of edges  $E \subset V \times V$ . As in Lenkoski (2013), we slightly abuse notation and write  $(i, j) \in G$  for  $(i, j) \in E$ , i.e. when vertices  $i$  and  $j$  are connected in  $G$ . We aim to infer  $G$  given an  $n \times p$  data matrix  $Y$  with  $n \geq 1$  independent rows distributed according to  $\mathcal{N}(0, K^{-1})$  for a precision matrix  $K \in M^+$ , where  $M^+$  is the set of  $p \times p$  symmetric, positive-definite matrices. Graph  $G$  constrains  $K$  in that  $K_{ij} = 0$  if  $(i, j) \notin G$ . Thus,  $K \in M^+(G)$ , where  $M^+(G) \subset M^+$  is the cone of matrices  $K \in M^+$  with  $K_{ij} = 0$  for  $(i, j) \notin G$ .

Following the notation in Section 2,  $x = (K, G)$  and  $y = Y$ . Notice that we are required to include  $K$  into  $x$  as only then  $p(y | x)$  is analytically available. We get  $p(y | x) = p(Y | K, G) = p(Y | K) = (2\pi)^{-np/2} |K|^{n/2} \exp(-\frac{1}{2} \langle K, U \rangle)$  where  $U = Y^\top Y$  is the scatter matrix and  $\langle K, U \rangle = \text{tr}(K^\top U)$  the trace inner product. A conjugate prior for  $K$  conditional on  $G$  is the  $G$ -Wishart distribution  $\mathcal{W}_G(\delta, D)$  (Roverato, 2002) with density

$$p(K | G) = \frac{1}{I_G(\delta, D)} |K|^{\delta/2-1} \exp\left(-\frac{1}{2} \langle K, D \rangle\right), \quad K \in M^+(G),$$

parametrised by  $\delta > 2$  and a positive-definite rate matrix  $D$ . The normalising constant  $I_G(\delta, D)$  does not have an analytical form for general non-decomposable  $G$  (Uhler et al., 2018). We henceforth choose  $\delta = 3$  in agreement with previous work (Jones et al., 2005; Lenkoski, 2013; Tan et al., 2017). Due to conjugacy,  $K | G, Y \sim \mathcal{W}_G(\delta + n, D^*)$  where  $D^* = D + U$ . Since the objective is inference on  $G$ , one would like to compute the posterior

$$\begin{aligned} p(G | Y) &\propto p(G) p(Y | G) = p(G) \int_{M^+(G)} p(Y | K, G) p(K | G) dK \\ &\propto p(G) \frac{I_G(\delta + n, D^*)}{I_G(\delta, D)}, \end{aligned} \quad (3)$$

with  $p(G)$  the prior on  $G$ .

As the normalising constant  $I_G$  is not analytically available in general, some approximation is required. Standard approaches apply Monte Carlo or Laplace approximation of  $p(G | Y)$  (Atay-Kayis & Massam, 2005; Tan et al., 2017). Recent work avoids approximation of normalising constants via careful MCMC constructions. See Wang & Li (2012); Cheng & Lenkoski (2012); Lenkoski (2013). Our methodology falls in this latter direction of research. Compared to Wang & Li (2012); Cheng & Lenkoski (2012), our MCMC samples directly from  $G$ -Wishart distributions, rather than preserving them, to improve mixing. Our MCMC sampler is very similar to the one in Lenkoski (2013), with the exception of sampling elements of the involved precision matrices directly from the full conditional distribution, rather than applying a Metropolis-within-Gibbs step. Such a choice removes a tuning parameter.

We use a size-based prior (Armstrong et al., 2009, Section 2.4) for  $G$ . That is,  $p(G)$  is the induced marginal of a joint prior distribution on  $G$  and the number of edges  $n_e = |E|$  such that the prior on  $G$  given  $n_e$  is uniform,  $p(G | n_e) \propto 1$ . For

$n_e$ , we chose a truncated geometric distribution with success probability  $1/(p+1)$ , i.e.  $p(n_e) \propto \{p/(p+1)\}^{n_e}$ ,  $n_e = 0, 1, \dots, p(p-1)/2$ . This choice completes the prior specification for  $G$  and induces sparsity. The success probability is such that the mean of the non-truncated geometric law equals the number of vertices  $p$ . Prior elicitation based on the sparsity constraint that the prior mean of  $n_e$  equals  $p$  has also been used with independent-edge priors (Jones et al., 2005, Section 2.4).

## 5.2 Inner MCMC step

We set up an MCMC step with  $p(x | y) = p(K, G | Y)$  as invariant distribution. The corresponding MCMC step for the tempered density  $p_\alpha(x | y)$ ,  $\alpha \in (0, 1]$ , required for Algorithm 6, follows by replacing  $n$  and  $U$  by  $\alpha n$  and  $\alpha U$ , respectively, since  $p(y | x)^\alpha = (2\pi)^{-\alpha np/2} |K|^{\alpha n/2} \exp(-\frac{1}{2} \langle K, \alpha U \rangle)$ . We make use of the algorithm for sampling from a  $G$ -Wishart law introduced in Lenkoski (2013, Section 2.4). Thus, we can sample from  $K | G, Y \sim \mathcal{W}_G(\delta + n, D^*)$ . It remains to derive an MCMC transition that preserves  $p(G | Y)$ , as samples of  $G$  can be extended to  $x = (K, G)$  by generating  $K | G, Y$ .

We consider the double reversible jump approach from Lenkoski (2013) and apply the node reordering from Cheng & Lenkoski (2012, Section 2.2) to obtain an MCMC step with no tuning parameters. The MCMC step is a Metropolis-Hastings algorithm on an enlarged space that bypasses the evaluation of the intractable normalisation constants  $I_G(\delta, D)$  and  $I_G(\delta + n, D^*)$  in the target distribution (3). It is a combination of ideas from the PAS algorithm of Godsill (2001), which avoids the evaluation of  $I_G(\delta + n, D^*)$ , and the exchange algorithm of Murray et al. (2006), which sidesteps evaluation of  $I_G(\delta, D)$ . We will give a brief presentation of the MCMC kernel that we are using as it does not coincide with approaches that have appeared in the literature.

To attain the objective of suppressing the normalising constants in the method, one works with a posterior on an extended space, defined via the directed acyclic graph in Figure 3. The left side of the graph gives rise to the original posterior  $p(G)p(K | G)p(Y | K)$ . Denote by  $\tilde{G}$  the proposed graph, with law  $q(\tilde{G} | G)$ . Lenkoski (2013) chooses a pair of vertices  $(i, j)$  in  $G$ ,  $i < j$ , at random and applies a reversal, i.e.  $(i, j) \in \tilde{G}$  if and only if  $(i, j) \notin G$ . The downside is that the probability of removing an edge is proportional to the number of edges in  $G$ , which is typically small. Instead, we consider the method in Dobra et al. (2011, Equation A.1) that also applies the reversal, but chooses  $(i, j)$  so that the probabilities of adding and removing an edge are equal.

We reorder the nodes of  $G$  and  $\tilde{G}$  so that the edge that has been altered is  $(p-1, p)$ , similarly to Cheng & Lenkoski (2012, Section 2.2). Given  $\tilde{G}$ , the graph in Figure 3 contains a final node that refers to the conditional distribution of  $p(\tilde{K} | \tilde{G})$  which coincides with the  $G$ -Wishart prior  $p(K | G)$ . Consider the upper triangular Cholesky decomposition  $\Phi$  of  $K$  so that  $\Phi^\top \Phi = K$ . Let  $\Phi_{-f} = \Phi \setminus \Phi_{p-1, p}$ . We work with the transform  $K \leftrightarrow \Phi = (\Phi_{-f}, \Phi_{p-1, p})$ . We apply a similar decomposition for  $\tilde{K}$ , and obtain the transform  $\tilde{K} \leftrightarrow \tilde{\Phi} = (\tilde{\Phi}_{-f}, \tilde{\Phi}_{p-1, p})$ .

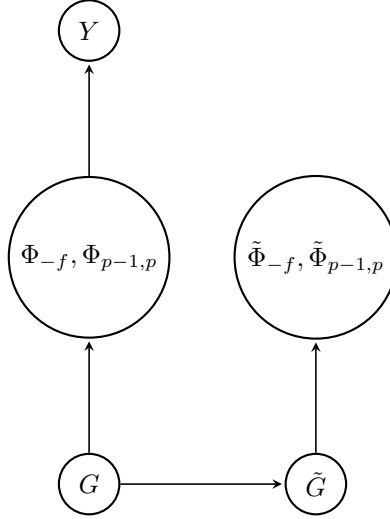


Figure 3: The enlarged hierarchical model giving rise to a posterior on an extended space that will be preserved by our MCMC kernel. The construction aims at: i) removing the requirement for calculation of intractable normalising constants; ii) avoiding introducing tuning parameters. The main text defines  $\Phi = (\Phi_{-f}, \Phi_{p-1,p})$  and  $\tilde{\Phi} = (\tilde{\Phi}_{-f}, \tilde{\Phi}_{p-1,p})$ .

We can now define the target posterior on the extended space as

$$p(G, \tilde{G}, \Phi_{p-1,p}, \tilde{\Phi}_{p-1,p} \mid \Phi_{-f}, \tilde{\Phi}_{-f}, Y) \propto p(G) q(\tilde{G} \mid G) p(\Phi \mid G) p(\tilde{\Phi} \mid \tilde{G}) p(Y \mid \Phi).$$

Given a graph  $G$ , the current state on the extended space comprises of

$$(G, \tilde{G}, \Phi_{-f}, \Phi_{p-1,p}, \tilde{\Phi}_{-f}, \tilde{\Phi}_{p-1,p}), \quad (4)$$

with  $\tilde{G} \sim q(\tilde{G} \mid G)$ , and  $\Phi, \tilde{\Phi}$  obtained from the Cholesky decomposition of the precision matrices  $K \sim \mathcal{W}_G(\delta + n, D + U)$ ,  $\tilde{K} \sim \mathcal{W}_{\tilde{G}}(\delta, D)$ , respectively. Notice that the rows and columns of  $D$  and  $U$  have been accordingly reordered to agree with the re-arrangement of the nodes we describe above. Consider the scenario with the proposed graph  $\tilde{G}$  having one more edge than  $G$ . Given the current state in (4), the algorithm proposes a move to the state

$$(\tilde{G}, G, \Phi_{-f}, \Phi_{p-1,p}^{\text{pr}}, \tilde{\Phi}_{-f}, \tilde{\Phi}_{p-1,p}^{\text{pr}}).$$

The value  $\Phi_{p-1,p}^{\text{pr}}$  is sampled from the conditional law of  $\Phi_{p-1,p} \mid \Phi_{-f}, Y$ .

We provide here some justification for the above construction. The main points are the following: (i) the proposal corresponds to an exchange of  $G \leftrightarrow \tilde{G}$ , coupled with a suggested position for the newly ‘freed’ matrix element  $\Phi_{p-1,p}^{\text{pr}}$ ; (ii) from standard properties of the general exchange algorithm, switching the

position of  $G, \tilde{G}$  will cancel out the normalising constants of the  $G$ -Wishart prior from the acceptance probability; iii) the normalising constants of the  $G$ -Wishart posterior never appear, as the precision matrices are not integrated out.

Appendix C derives that

$$\Phi_{p-1,p} \mid \Phi_{-f}, Y \sim \mathcal{N} \left( \frac{-D_{p-1,p}^* \Phi_{p-1,p-1}}{D_{p,p}^*}, \frac{1}{D_{p,p}^*} \right). \quad (5)$$

This avoids the tuning of a step-size parameter arising in the Gaussian proposal of Lenkoski (2013, Section 3.2). The variable  $\tilde{\Phi}_{p-1,p}^{\text{pr}}$  is not free, due to the edge  $(p-1, p)$  assumed being removed, and is given as (Roverato, 2002, Equation 10)

$$\tilde{\Phi}_{p-1,p}^{\text{pr}} = - \sum_{i=1}^{p-2} \tilde{\Phi}_{i,p-1} \tilde{\Phi}_{ip} / \tilde{\Phi}_{p-1,p-1}.$$

The acceptance probability of the proposal is given in Step 6 of the complete MCMC transition shown in Algorithm 7 for exponent  $\epsilon = 1$ . In the opposite scenario when an edge is removed from  $G$ , then, after again re-ordering the nodes, the proposal  $\tilde{\Phi}_{p-1,p}^{\text{pr}}$  is sampled from

$$\tilde{\Phi}_{p-1,p} \mid \tilde{\Phi}_{-f} \sim \mathcal{N} \left( \frac{-D_{p-1,p} \tilde{\Phi}_{p-1,p-1}}{D_{p,p}}, \frac{1}{D_{p,p}} \right)$$

whereas we fix  $\Phi_{p-1,p}^{\text{pr}} = - \sum_{i=1}^{p-2} \Phi_{i,p-1} \Phi_{ip} / \Phi_{p-1,p-1}$ . The corresponding acceptance probability for the proposed move is again as in Step 6 of Algorithm 7, but now for  $\epsilon = -1$ . We do not make use of prime-subgraph decomposition (Wang & Carvalho, 2010) in the execution of the algorithm, as it does not provide computational benefits for the number of nodes  $p$  we consider in this work.

### 5.3 Further algorithmic specifications

#### Rejection sampling with $\alpha_0 > 0$

We set  $\alpha_0 > 0$  and resort to rejection sampling with the prior  $p(x)$  as proposal to sample from  $\pi_{\alpha_1}(x)$  in Step 1 of Algorithm 2. This reduces the computational cost for the overall SMC algorithm considerably in our applications, due to the prior  $p(G)$  being diffuse: Algorithm 7 changes at most one edge of the graph in each step such that a large number of steps  $m_1$  are required for effective diversification of particles for small  $\alpha_1$  for which  $\pi_{\alpha_1}(x) \approx p(x)$ . This implementation of the  $m_1$  MCMC steps then dominates the computational cost. Setting  $\alpha_0 > 0$  induces a larger  $\alpha_1$  and a much smaller  $m_1$ .

The maximum likelihood estimate of  $K$  is  $\arg \max_K p(Y \mid K) = nU^{-1}$ . So, the acceptance probability of the rejection sampler follows as

$$\begin{aligned} \frac{p(y \mid x_0^i)^{\alpha_0}}{\sup_{x \in \mathcal{X}} p(y \mid x)^{\alpha_0}} &= \frac{p(Y \mid K_0^i)^{\alpha_0}}{\sup_{K \in M^+(G)} p(Y \mid K)^{\alpha_0}} \\ &= (|K_0^i| |U|)^{n\alpha_0/2} \exp \left[ \frac{\alpha_0}{2} \{ np(1 - \log n) - \langle K_0^i, U \rangle \} \right]. \end{aligned}$$

---

**Algorithm 7** Inner MCMC mutation for the Gaussian graphical model.

---

Input: Graph  $G$ .

1. (a) If  $G$  is complete or empty, sample  $(i, j)$ ,  $i < j$ , uniformly from the edges in  $G$  or the edges not in  $G$ , respectively.  
 (b) Else, sample  $(i, j)$ ,  $i < j$ , as follows: w.p.  $1/2$ , uniformly from the edges in  $G$ ; w.p.  $1/2$ , uniformly from the edges not in  $G$ .
2. Reorder the nodes in  $G$  so that the  $i$ -th and  $j$ -th nodes become the  $(p-1)$ -th and  $p$ -th nodes, respectively. Rearrange  $D$  and  $D^*$  accordingly.
3. Let  $\tilde{G}$  be as  $G$  except for edge  $(p-1, p)$ , with  $(p-1, p) \in \tilde{G}$  if and only if  $(p-1, p) \notin G$ .
4. Sample  $K \sim \mathcal{W}_G(\delta + n, D^*)$ ,  $\tilde{K} \sim \mathcal{W}_{\tilde{G}}(\delta, D)$ . Compute the corresponding upper triangular Cholesky decompositions  $\Phi$ ,  $\tilde{\Phi}$ .
5. Fix  $\Phi_{-f} = \Phi \setminus \Phi_{p-1,p}$  and  $\tilde{\Phi}_{-f} = \tilde{\Phi} \setminus \tilde{\Phi}_{p-1,p}$ .  
 (a) If  $(p-1, p) \notin G$ , sample the proposal

$$\Phi_{p-1,p}^{\text{Pr}} \mid \Phi_{-f}, Y \sim \mathcal{N}(-D_{p-1,p}^* \Phi_{p-1,p-1} / D_{p,p}^*, 1/D_{p,p}^*)$$

$$\text{and set } \tilde{\Phi}_{p-1,p}^{\text{Pr}} = -\sum_{i=1}^{p-2} \tilde{\Phi}_{i,p-1} \tilde{\Phi}_{ip} / \tilde{\Phi}_{p-1,p-1}.$$

- (b) If  $(p-1, p) \in G$ , sample the proposal

$$\tilde{\Phi}_{p-1,p}^{\text{Pr}} \mid \tilde{\Phi}_{-f} \sim \mathcal{N}(-D_{p-1,p} \tilde{\Phi}_{p-1,p-1} / D_{p,p}, 1/D_{p,p})$$

$$\text{and set } \Phi_{p-1,p}^{\text{Pr}} = -\sum_{i=1}^{p-2} \Phi_{i,p-1} \Phi_{ip} / \Phi_{p-1,p-1}.$$

6. Accept the proposed move from state  $(G, \tilde{G}, \Phi_{-f}, \Phi_{p-1,p}, \tilde{\Phi}_{-f}, \tilde{\Phi}_{p-1,p})$  to state  $(\tilde{G}, G, \Phi_{-f}, \Phi_{p-1,p}, \tilde{\Phi}_{-f}, \tilde{\Phi}_{p-1,p}^{\text{Pr}})$  w.p.  $1 \wedge R$ , for  $R$  equal to

$$\frac{p(\tilde{G})q(G|\tilde{G})}{p(G)q(\tilde{G}|G)} \exp \left\{ -\frac{1}{2} \langle K^{\text{Pr}} - K, D^* \rangle - \frac{1}{2} \langle \tilde{K}^{\text{Pr}} - \tilde{K}, D \rangle \right\} \\ \times \left[ \frac{\Phi_{p-1,p-1} \sqrt{D_{p,p}}}{\tilde{\Phi}_{p-1,p-1} \sqrt{D_{p,p}^*}} \exp \left\{ \frac{D_{p,p}}{2} (\tilde{\Phi}_{p-1,p}^{\text{Pr}} - \tilde{\theta})^2 - \frac{D_{p,p}^*}{2} (\Phi_{p-1,p}^{\text{Pr}} - \theta)^2 \right\} \right]^\epsilon,$$

for  $\tilde{\theta} = -D_{p-1,p} \tilde{\Phi}_{p-1,p-1} / D_{p,p}$  and  $\theta = -D_{p-1,p}^* \Phi_{p-1,p-1} / D_{p,p}^*$ . Here,  $K^{\text{Pr}}$  (resp.  $\tilde{K}^{\text{Pr}}$ ) denotes the precision with upper triangular Cholesky decomposition given by the synthesis of  $\Phi_{-f}, \Phi_{p-1,p}^{\text{Pr}}$  (resp.  $\tilde{\Phi}_{-f}, \tilde{\Phi}_{p-1,p}^{\text{Pr}}$ ), and  $\epsilon = -1$  if  $(p-1, p) \in G$ , else  $\epsilon = 1$ .

7. Revert the reordering from Step 2. Return  $\tilde{G}$  if the proposed move at Step 6 is accepted, else return  $G$ .

Output: MCMC update for graph  $G$  such that the invariant distribution is the target posterior  $p(G \mid Y)$ .

---

We choose  $\alpha_0$  to achieve an acceptance rate of  $a = 1/50$ . Specifically, we draw  $N_0/a$  particles from the prior  $p(x)$  and set  $\alpha_0$  to the largest value such that  $N_0$  of these particles are accepted.

### PIMH vs conditional SMC

The main challenge for the class of Gaussian graphical models is the effective coupling of the outer MCMC chain so that the size of the meeting times  $\tau$  is not large. Following the discussion in Section 4, PIMH yields smaller  $\tau$  than conditional SMC. We therefore use Algorithm 6 with  $\rho = 0$  here.

## 5.4 Data description

We consider metabonomic data as an application of Gaussian graphical models. The sample consists of  $n = 471$  six-year-old children from the Growing Up in Singapore Towards healthy Outcomes (GUSTO) study (Soh et al., 2014). Measurements are taken from blood serum samples via nuclear magnetic resonance to obtain metabolic phenotypes. Specifically, the levels of certain metabolites, which are low-molecular-weight molecules involved in metabolism, are measured. Examples of metabolites are cholesterol, fatty acids and glucose. See Soinen et al. (2009) for a description of the measurement process. We focus on a set of 35 metabolites. Thus, the  $n \times p$  data matrix  $Y$  consists of  $p = 35$  metabolite levels from  $n = 471$  children. We quantile normalise the metabolites such that they marginally follow a standard Gaussian distribution.

## 5.5 Results

The univariate statistics of  $x$  used to determine the number of MCMC steps  $m_s$  are the log-likelihood  $f_1(x) = \log\{p(y | x)\}$  and the number of edges  $f_2(x) = |E|$ . The adaptation results in  $S = 165$  temperatures with  $m_s$  varying from 1 to 14 and a mean of 6 for  $s > 1$  and  $m_1 = 15$ . Indeed, having  $\alpha_0 > 0$  ensures that the tempered posterior  $\pi_{\alpha_1}(x)$  is further away from the uninformative prior  $p(x)$  such that the number of MCMC steps for sufficient diversification of particles is limited.

Algorithm 6 is run for  $l = 40$  MCMC steps with  $N = 10^3$  particles, until the chains meet or when the time budget is up, whichever comes first. We do this repeatedly across 16 CPU cores simultaneously and independently. Our time budget is 72 hours. This results in 30 finished runs of Algorithm 6 and 16 incomplete runs that are cut short due to running out of time. Such incomplete runs introduce a bias, though this bias decays exponentially with the time budget as discussed in Section 3.3 of Jacob et al. (2020b). Of the finished 30 runs, 19 meet in  $\tau = 1$  step and the largest observed  $\tau$  is 10.

We use these runs to obtain multiple unbiased estimates based on (2) with  $k = 7$  and  $l = 40$  where  $h(x)$  is chosen to estimate the posterior edge inclusion probabilities, i.e. the posterior probability of whether an edge is included in the graph  $G$ . Figure 4 shows the estimates. Since they result from averaging

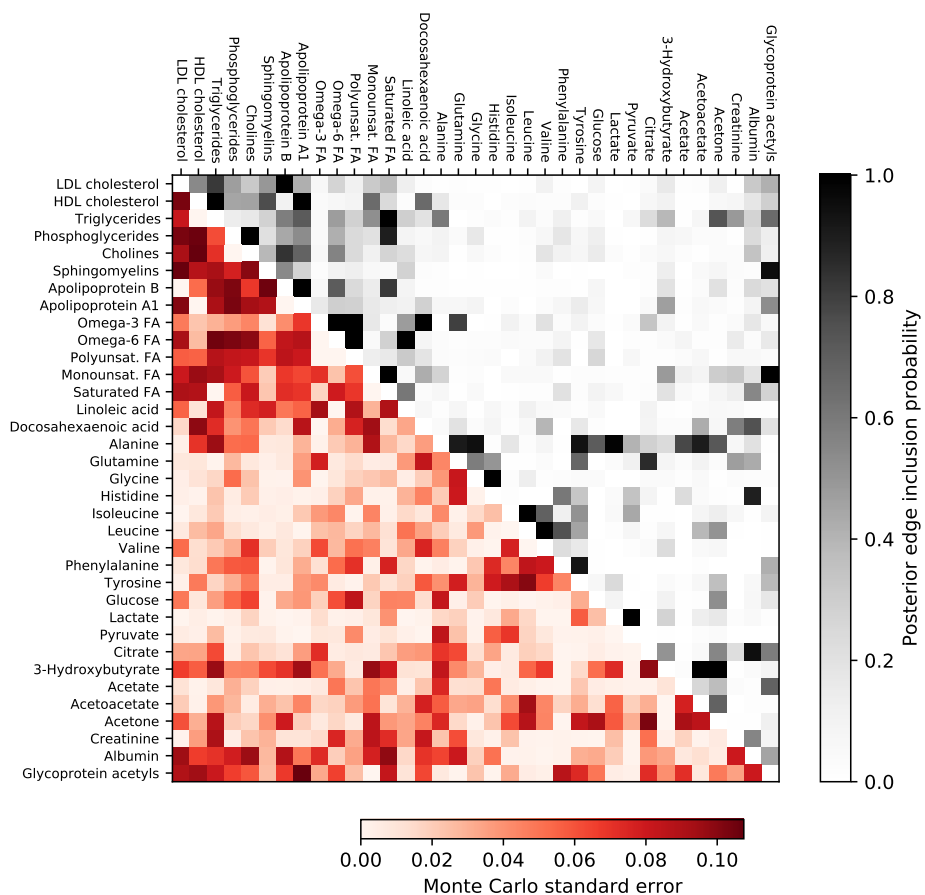


Figure 4: Posterior edge inclusion probabilities (upper triangle) and their Monte Carlo standard errors (lower triangle) resulting from coupled particle MCMC for the Gaussian graphic model fit on the metabolite data. LDL, HDL and FA stand for low-density lipoprotein, high-density lipoprotein and fatty acids, respectively.



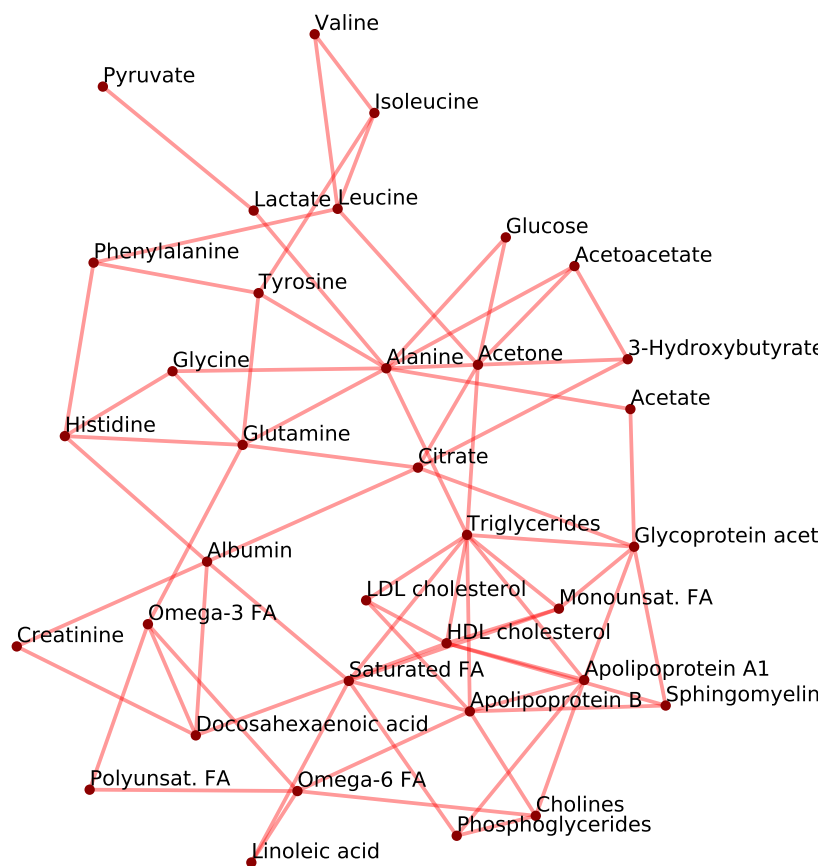


Figure 5: The median probability graph resulting from coupled particle MCMC for the Gaussian graphic model fit on the metabolite data. LDL, HDL and FA stand for low-density lipoprotein, high-density lipoprotein and fatty acids, respectively.

independent and unbiased estimators, we can also estimate their Monte Carlo error. Figure 4 confirms that the chosen time budget is sufficient to achieve a usable posterior approximation with the standard errors maxing out at 0.11. Appendix D compares these probabilities with estimates from running SMC once with a large number of particles. Figure 5 contains the median probability graph, i.e. the graph which includes edges with a posterior inclusion probability greater than 0.5.

## 6 Discussion

In this work, we show how coupled particle MCMC can yield effective unbiased posterior estimation. It comes with attractive theoretical properties owing to the literature on state-space models. Gaussian graphical models provide an example where a good coupling of the MCMC is hard while coupled particle MCMC produces Markov chains that tend to couple quickly.

Major empirical and theoretical improvements in coupling have been reported for the ancestral and backward sampling modifications to conditional SMC (Chopin & Singh, 2015; Jacob et al., 2020a; Lee et al., 2020). For instance, Lee et al. (2020, Theorem 11) show that the one-step meeting probability analysed in Proposition 1 does not vanish if  $N = \mathcal{O}(S)$  for conditional SMC with backward sampling. Unfortunately, these modifications can usually not be used in our scenario as the transition densities in the Feynman-Kac model resulting from taking  $m_s$  inner MCMC steps are often intractable.

The use of SMC adds computational cost compared to running MCMC by itself. For instance, a single step in the outer MCMC defined by PIMH or conditional SMC involves  $N \sum_{s=1}^S m_s$  inner MCMC steps. This extra computational cost is amenable to parallelization due to the embarrassingly parallel nature of the particles in SMC. Moreover, the extra computational effort results in more accurate Monte Carlo estimates due to Rao-Blackwellization across the  $N$  particles. One of the main contributions of this work is to gain further insight into these novel computational strategies. For instance, Section 4 shows that it depends on the shape of the posterior at hand whether the extra computational effort deriving from the SMC is ultimately worth it.

## References

- ANDRIEU, C., DOUCET, A. & HOLENSTEIN, R. (2010). Particle Markov chain Monte Carlo methods. *Journal of the Royal Statistical Society: Series B (Statistical Methodology)* **72**, 269–342.
- ANDRIEU, C., LEE, A. & VIHOLA, M. (2018). Uniform ergodicity of the iterated conditional SMC and geometric ergodicity of particle Gibbs samplers. *Bernoulli* **24**, 842–872.
- ARMSTRONG, H., CARTER, C. K., WONG, K. F. K. & KOHN, R. (2009).

- Bayesian covariance matrix estimation using a mixture of decomposable graphical models. *Statistics and Computing* **19**, 303–316.
- ATAY-KAYIS, A. & MASSAM, H. (2005). A Monte Carlo method for computing the marginal likelihood in nondecomposable Gaussian graphical models. *Biometrika* **92**, 317–335.
- BESKOS, A., CRISAN, D., JASRA, A. et al. (2014). On the stability of sequential Monte Carlo methods in high dimensions. *The Annals of Applied Probability* **24**, 1396–1445.
- BHADRA, A., DATTA, J., POLSON, N. G. & WILLARD, B. (2019). Lasso meets horseshoe: A survey. *Statistical Science* **34**, 405–427.
- BISWAS, N., BHATTACHARYA, A., JACOB, P. E. & JOHNDROW, J. E. (2020). Coupled Markov chain Monte Carlo for high-dimensional regression with Half-t priors. ArXiv:2012.04798v1.
- CARVALHO, C. M., POLSON, N. G. & SCOTT, J. G. (2009). Handling sparsity via the horseshoe. In *Proceedings of the Twelfth International Conference on Artificial Intelligence and Statistics*, D. van Dyk & M. Welling, eds., vol. 5 of *Proceedings of Machine Learning Research*. Hilton Clearwater Beach Resort, Clearwater Beach, Florida USA: PMLR.
- CHENG, Y. & LENKOSKI, A. (2012). Hierarchical Gaussian graphical models: Beyond reversible jump. *Electronic Journal of Statistics* **6**, 2309–2331.
- CHOPIN, N. & PAPASPILIOPOULOS, O. (2020). *An Introduction to Sequential Monte Carlo*. Springer International Publishing.
- CHOPIN, N. & SINGH, S. S. (2015). On particle Gibbs sampling. *Bernoulli* **21**, 1855–1883.
- DEL MORAL, P. (2004). *Feynman-Kac Formulae: Genealogical and Interacting Particle Systems with Applications*. Springer, New York.
- DEL MORAL, P., DOUCET, A. & JASRA, A. (2006). Sequential Monte Carlo samplers. *Journal of the Royal Statistical Society: Series B (Statistical Methodology)* **68**, 411–436.
- DEMPSTER, A. P. (1972). Covariance selection. *Biometrics* **28**, 157.
- DOBRA, A., LENKOSKI, A. & RODRIGUEZ, A. (2011). Bayesian inference for general Gaussian graphical models with application to multivariate lattice data. *Journal of the American Statistical Association* **106**, 1418–1433.
- GLYNN, P. W. & RHEE, C.-H. (2014). Exact estimation for Markov chain equilibrium expectations. *Journal of Applied Probability* **51**, 377–389.

- GODSILL, S. J. (2001). On the relationship between Markov chain Monte Carlo methods for model uncertainty. *Journal of Computational and Graphical Statistics* **10**, 230–248.
- JACOB, P. E., LINDSTEN, F. & SCHÖN, T. B. (2020a). Smoothing with couplings of conditional particle filters. *Journal of the American Statistical Association* **115**, 721–729.
- JACOB, P. E., O’LEARY, J. & ATCHADÉ, Y. F. (2020b). Unbiased Markov chain Monte Carlo methods with couplings. *Journal of the Royal Statistical Society: Series B (Statistical Methodology)* **82**, 543–600.
- JASRA, A., KAMATANI, K., LAW, K. J. H. & ZHOU, Y. (2017). Multilevel particle filters. *SIAM Journal on Numerical Analysis* **55**, 3068–3096.
- JASRA, A., STEPHENS, D. A., DOUCET, A. & TSAGARIS, T. (2010). Inference for Lévy-driven stochastic volatility models via adaptive sequential Monte Carlo. *Scandinavian Journal of Statistics* **38**, 1–22.
- JONES, B., CARVALHO, C., DOBRA, A., HANS, C., CARTER, C. & WEST, M. (2005). Experiments in stochastic computation for high-dimensional graphical models. *Statistical Science* **20**, 388–400.
- KANTAS, N., BESKOS, A. & JASRA, A. (2014). Sequential Monte Carlo methods for high-dimensional inverse problems: A case study for the Navier–Stokes equations. *SIAM/ASA Journal on Uncertainty Quantification* **2**, 464–489.
- LAURITZEN, S. L. (1996). *Graphical Models*. Oxford Statistical Science Series. The Clarendon Press, Oxford University Press, New York.
- LEE, A., SINGH, S. S. & VIHOLA, M. (2020). Coupled conditional backward sampling particle filter. *Annals of Statistics* **48**, 3066–3089.
- LENKOSKI, A. (2013). A direct sampler for G-Wishart variates. *Stat* **2**, 119–128.
- MIDDLETON, L., DELIGIANNIDIS, G., DOUCET, A. & JACOB, P. E. (2019). Unbiased smoothing using particle independent Metropolis-Hastings. In *Proceedings of Machine Learning Research*, K. Chaudhuri & M. Sugiyama, eds., vol. 89 of *Proceedings of Machine Learning Research*. PMLR.
- MURRAY, I., GHAHRAMANI, Z. & MACKAY, D. J. C. (2006). MCMC for doubly-intractable distributions. In *Proceedings of the Twenty-Second Conference on Uncertainty in Artificial Intelligence, UAI’06*. Arlington, Virginia, USA: AUAI Press.
- ROSENTHAL, J. S. (1997). Faithful couplings of Markov chains: Now equals forever. *Advances in Applied Mathematics* **18**, 372–381.
- ROVERATO, A. (2002). Hyper inverse Wishart distribution for non-decomposable graphs and its application to Bayesian inference for Gaussian graphical models. *Scandinavian Journal of Statistics* **29**, 391–411.

- SOH, S.-E., TINT, M. T., GLUCKMAN, P. D., GODFREY, K. M., RIFKIN-GRABOI, A., CHAN, Y. H., STÜNKEL, W., HOLBROOK, J. D., KWEK, K., CHONG, Y.-S., SAW, S. M. & THE GUSTO STUDY GROUP (2014). Cohort profile: Growing up in Singapore towards healthy outcomes (GUSTO) birth cohort study. *International Journal of Epidemiology* **43**, 1401–1409.
- SOININEN, P., KANGAS, A. J., WÜRTZ, P., TUKIAINEN, T., TYNKKYNNEN, T., LAATIKAINEN, R., JÄRVELIN, M.-R., KÄHÖNEN, M., LEHTIMÄKI, T., VIIKARI, J., RAITAKARI, O. T., SAVOLAINEN, M. J. & ALA-KORPELA, M. (2009). High-throughput serum NMR metabonomics for cost-effective holistic studies on systemic metabolism. *The Analyst* **134**, 1781.
- STATISTICAT, LLC. (2020). *LaplacesDemon: Complete Environment for Bayesian Inference*. R package version 16.1.4.
- TAN, L. S. L., JASRA, A., DE IORIO, M. & EBBELS, T. M. D. (2017). Bayesian inference for multiple Gaussian graphical models with application to metabolic association networks. *The Annals of Applied Statistics* **11**, 2222–2251.
- UHLER, C., LENKOSKI, A. & RICHARDS, D. (2018). Exact formulas for the normalizing constants of Wishart distributions for graphical models. *The Annals of Statistics* **46**, 90–118.
- WANG, H. & CARVALHO, C. M. (2010). Simulation of hyper-inverse Wishart distributions for non-decomposable graphs. *Electronic Journal of Statistics* **4**, 1470–1475.
- WANG, H. & LI, S. Z. (2012). Efficient Gaussian graphical model determination under G-Wishart prior distributions. *Electronic Journal of Statistics* **6**, 168–198.

## A Systematic resampling

Algorithms 8 through 10 detail the systematic resampling methods used for the empirical results derived from Algorithm 6. They involve the floor function denoted by  $\lfloor x \rfloor$ , i.e.,  $\lfloor x \rfloor$  is the largest integer for which  $\lfloor x \rfloor \leq x$ .

## B Proofs for Section 3

Our results derive from Lee et al. (2020). They consider a smoothing set-up which maps to our context of approximating a general posterior  $\pi(x)$  using adaptive SMC. Specifically, their target density is (Lee et al., 2020, Equation 1)

$$\Pi(x_{0:S}) \propto M_0(x_0) G_0(x_0) \prod_{s=1}^S M_s(x_{s-1}, x_s) G_s(x_{s-1}, x_s). \quad (6)$$

---

**Algorithm 8** Systematic resampling.

---

Input: Probability vector  $p_{1:N}$  and  $U \in [0, 1]$ .

1. Compute the cumulative sums  $v_i = N \sum_{j=1}^i p_j$ ,  $i = 1, \dots, N$ .
2. Let  $j = 1$ .
3. For  $i = 1, \dots, N$ ,
  - (a) While  $v_j < U$ , do  $j = j + 1$ .
  - (b) Let  $A_i = j$  and  $U = U + 1$ .

Output: A vector of  $N$  random indices  $A$  such that, if the input  $U \sim \mathcal{U}(0, 1)$ , then the expectation of the frequency of any index  $i$  equals  $Np_i$ .

---

---

**Algorithm 9** (Chopin & Singh, 2015, Algorithm 4) Conditional systematic resampling.

---

Input: Probability vector  $p_{1:N}$ .

1. Compute  $r = Np_1 - \lfloor Np_1 \rfloor$  and sample

$$U \sim \begin{cases} \mathcal{U}(0, Np_1), & r \leq 0 \\ \frac{r(\lfloor Np_1 \rfloor + 1)}{Np_1} \mathcal{U}(0, r) + \frac{Np_1 - r(\lfloor Np_1 \rfloor + 1)}{Np_1} \mathcal{U}(r, 1), & r > 0 \end{cases}$$

2. Obtain a vector of indices  $B$  by running Algorithm 8 with  $p_{1:N}$  and  $U$  as input.
3. Draw  $A$  uniformly from all cycles of  $B$  that yield  $A_1 = 1$ .

Output: A vector of  $N$  random indices  $A$  with  $A_1 = 1$ .

---

---

**Algorithm 10** Coupled conditional systematic resampling.

---

Input: Probability vectors  $p_{1:N}, \bar{p}_{1:N}$ .

1. Generate  $B$  and  $\bar{B}$  by running the first two steps of Algorithm 9 with  $p_{1:N}$  and  $\bar{p}_{1:N}$  as input, respectively, using the same random numbers for each.
2. Construct a joint probability distribution on the cycles  $A$  and  $\bar{A}$  of  $B$  and  $\bar{B}$  for which  $A_1 = \bar{A}_1 = 1$  such that the marginal distributions are uniform:
  - (a) Calculate the overlap  $|\{i \in 1 : N \mid A_i = \bar{A}_i\}|$  for each pair of cycles with  $A_1 = \bar{A}_1 = 1$ .
  - (b) Iteratively assign the largest probability afforded by the constraint of uniform marginals to the pair with the highest overlap.
3. Draw  $A$  and  $\bar{A}$  from this joint distribution on cycles of  $B$  and  $\bar{B}$ .

Output: Vectors  $A, \bar{A}$  of  $N$  random indices with  $A_1 = \bar{A}_1 = 1$ .

---

In our context,  $M_0(x) = \pi_{\alpha_0}(x)$  is a tempered posterior,  $G_0(x) = p(y \mid x)^{\alpha_1 - \alpha_0}$  a tempered likelihood,  $M_s(x_{s-1}, x_s)$  the density of the Markov transition starting at  $x_{s-1}$  resulting from the  $m_s$  MCMC steps which are invariant w.r.t.  $\pi_{\alpha_s}(x)$  in Step 2c of Algorithm 2 for  $s = 1, \dots, S$ ,  $G_s(x_{s-1}, x_s) = p(y \mid x_s)^{\alpha_{s+1} - \alpha_s}$  a tempered likelihood for  $s = 1, \dots, S - 1$ , and  $G_S(x_{S-1}, x_S) = p(y \mid x_S)^{1 - \alpha_S}$  a tempered likelihood. Then, the coupled conditional particle filter in Algorithm 2 of Lee et al. (2020) reduces to the coupled conditional SMC in our Algorithm 4. Thus, the results in Lee et al. (2020) apply to Algorithm 4.

*Proof of Proposition 1.* Since  $G_s(x_{s-1}, x_s)$  does not depend on  $x_{s-1}$ , we can write  $G_s(x_{s-1}, x_s) = G(x_s)$  for  $s = 1, \dots, S$  as in Section 2 of Lee et al. (2020). Assumption 1, that  $p(y \mid x)$  is bounded, implies that  $G_s(x_s)$  is bounded for  $s = 0, \dots, S$ , which is Assumption 1 in Lee et al. (2020). Therefore, Theorem 8 of Lee et al. (2020) provides  $\Pr(x'_{0:S} = \bar{x}'_{0:S}) \geq N/(N + c)$ .

Part (iii) follows similarly to the proof for Theorem 10(iii) of Lee et al. (2020): We have  $\Pr(\tau > t) \leq \{1 - N/(N + c)\}^{t-1}$  for  $t \geq 1$ . Therefore,

$$E(\tau) = \sum_{t=0}^{\infty} \Pr(\tau > t) \leq 1 + \sum_{t=1}^{\infty} \Pr(\tau > t) \leq 1 + \sum_{t=1}^{\infty} \left(1 - \frac{N}{N + c}\right)^{t-1} = 2 + \frac{c}{N},$$

where the last equality follows from the geometric series formula  $\sum_{t=0}^{\infty} (1 - r)^t = 1/r$  for  $|r| < 1$ . Part (iii) implies Part (ii).  $\square$

*Proof of Proposition 2.* Theorem 10 of Lee et al. (2020) provides results for a statistic that we denote by  $h_{0:S} : \mathcal{X}^{S+1} \rightarrow \mathbb{R}$ . Consider  $h_{0:S}$  defined by  $h_{0:S}(x_{0:S}) = h(x_S)$  where  $h : \mathcal{X} \rightarrow \mathbb{R}$  is our statistic of interest. Then,  $h_{0:S}$  is bounded by Assumption 2. The marginal distribution of  $x_S$  under the density

on  $x_{0:S}$  in (6) is our posterior of interest  $\pi(x)$ . Consequently, the results for  $h_{0:S}$  in Theorem 10 of Lee et al. (2020) provide the required results for  $h$ .  $\square$

## C Proposal for precision matrices

This derivation is similar to Appendix A of Cheng & Lenkoski (2012). Assume that the edge  $(p-1, p)$  is in the proposed graph  $\tilde{G}$  but not in  $G$ . The prior on  $\tilde{\Phi}_{p-1,p} \mid \tilde{\Phi}_{-f}$  follows from Equation 2 of Cheng & Lenkoski (2012) as

$$p(\tilde{\Phi}_{p-1,p} \mid \tilde{\Phi}_{-f}, \tilde{G}) \propto \exp\left(-\frac{1}{2}\langle \tilde{\Phi}^\top \tilde{\Phi}, D \rangle\right).$$

The likelihood is

$$p(Y \mid \tilde{K}) \propto |\tilde{K}|^{n/2} \exp\left(-\frac{1}{2}\langle \tilde{K}, U \rangle\right).$$

Here,  $|\tilde{K}|$  does not depend on  $\tilde{\Phi}_{p-1,p}$  since  $|\tilde{K}| = |\tilde{\Phi}|^2 = (\prod_{i=1}^p \tilde{\Phi}_{ii})^2$ . Combining the previous two displays thus yields  $p(\tilde{\Phi}_{p-1,p} \mid \tilde{\Phi}_{-f}, Y) \propto \exp(-\langle \tilde{\Phi}^\top \tilde{\Phi}, D^* \rangle/2)$ . Dropping terms not involving  $\tilde{\Phi}_{p-1,p}$  yields (5).

## D Comparison with SMC for the metabolite application

We compare the results in Figure 4 with those from running the SMC in Algorithm 2 with a large number of particles  $N = 10^5$ . Comparing Figures 4 and 6 shows that the results are largely the same. The edge probabilities for which they differ substantially are harder to estimate according to the Monte Carlo standard errors from coupled particle SMC in Figure 4.



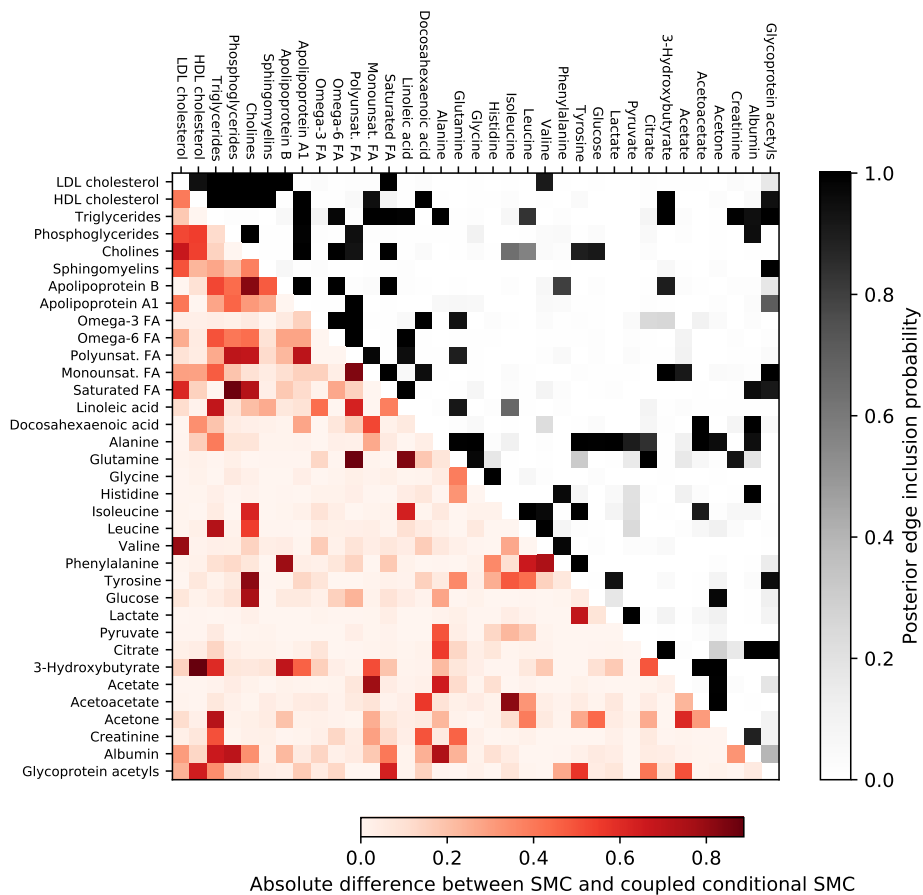


Figure 6: Posterior edge inclusion probabilities for the Gaussian graphic model fit on the metabolite data from SMC with  $N = 10^5$  particles (upper triangle) and their absolute difference from the estimates from coupled particle MCMC in Figure 4 (lower triangle). LDL, HDL and FA stand for low-density lipoprotein, high-density lipoprotein and fatty acids, respectively.